ACS OMEGA

http://pubs.acs.org/journal/acsodf

Article

Risk Assessment of Liquefied Petroleum Gas Explosion in a Limited Space

He Liang, Tao Wang,* Zhenmin Luo,* Xuqing Wang, Xiaofeng Kang, and Jun Deng

Cite This: *ACS Omega* 2021, 6, 24683−24692

Read Online

ACCESS | Metrics & More | Article Recommendations

ABSTRACT: In recent years, the explosion accidents of liquefied petroleum gas (LPG) have induced tremendous losses. To analyze the deflagration danger of LPG, the explosion pressure and flame propagation features of the premixed LPG−air mixture in a closed pipeline at increased initial pressures and temperatures were examined by the numerical method. It has been shown that with an increase in the initial temperature, the highest explosion pressure and explosion induction period decrease, while the maximum flame temperature increases. As the initial temperature rises, the formation of the tulip flame accelerates, and the depression of the flame front increases at the same time. The elevated initial pressure raises the highest explosion pressure and the maximum flame temperature. Nevertheless, when the initial pressure exceeds 0.5 MPa, its impact on the flame temperature slowly diminishes. In addition, the gray relational analysis approach was utilized to evaluate the correlation between the initial condition and the derived parameters. The findings indicate that the initial pressure exerts the largest influence on the four explosion parameters. The research finding is important for exposing the deflagration risk features of LPG under complicated working situations, evaluating the explosion risk of correlated procedures and devices, and formulating scientific and effective explosion-proof measures.

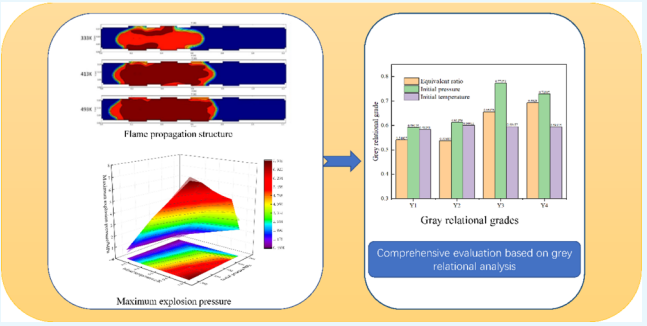

1. INTRODUCTION

Liquefied petroleum gas (LPG) is utilized extensively in chemical production and daily life[1−3] as an essential chemical raw material and a commercial cooking fuel. LPG, on the other hand, possesses flammable and explosive[4] properties. With its flammability, LPG is easily ignited, while it is leaking in the course of transportation and processing, thus causing fire or explosion,[5] especially in a confined space. The explosion of LPG is characterized by a high diffusion rate and rapid combustion speed.[6,7] The explosion disaster induced by LPG leakage has resulted in a high number of economic losses and casualties. From the previous research,[8−11] the flame propagation in the confined space is very complex, and the flame propagation in the confined space will undergo extremely complex morphological changes,[12−14] which will directly contribute to the acceleration of the flame and thus increase the explosion pressure.[15−18] Therefore, the building structure, production equipment, and human safety are compromised. At the same time, the study shows that the environmental conditions have a significant impact on the deflagration characteristics of flammable gas and steam,[19−23] so it is necessary to evaluate the explosion risk of LPG under different environmental conditions.

In recent years, many scholars have studied the combustion and explosion properties associated with LPG.[24,25] In general, the explosion features of combustible gases are affected by various factors, like initial temperature and pressure,[19,26,27] ignition energy,[9,28] obstacles,[17,29−32] and gas composition.[33−38] Using LPG−air and propane−air mixtures, Huzayyin et al.[24] estimated the laminar combustion rate and explosion index. The addition of CO_2 to LPG can lower the flammability limit, and the propagation flame can be controlled. The laminar combustion velocity reduces with an increase in the initial pressure and rises with an increase in the H_2 concentration[7,39] when hydrogen is introduced to LPG while under high pressure. The flame propagation of premixed LPG explosion in the tube was analyzed by Huo and Chow.[25] The two-zone LPG explosion experiment was conducted in a 25 m long pipe with a diameter of 2.6 m. It is observed that the flame propagation properties vary with time, and the flame propagation velocity at the explosion point is dependent on the turbulent combustion velocity and expansion ratio. Using a closed pipeline, Zhang et al.[40] investigated the explosion limit and flame propagation dynamics of dimethyl ether (DME)/

Received: June 30, 2021
Published: September 13, 2021

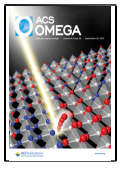

LPG premixed gas. The experimental findings depict that as the DME volume fraction increases, so does the explosion overpressure and maximum explosion pressure rise rate. Zhang et al.[1] analyzed the impact of barriers and concentrations on the explosion properties of LPG. It is concluded that the explosion overpressure and explosion temperature vary greatly with the LPG concentration in the air. The relationship linking the explosion temperature of the LPG−air mixture and the number of obstacles is very minimal when the plugging rate and concentration are constant.[41]

In summary, scholars have investigated the combustion and explosion features of LPG within various influencing factors, although prior studies are mostly focused on the normal temperature and pressure. The explosive characteristics of combustible gas are influenced by several factors, among which the initial pressure and the initial temperature are vital. During the processing and utilization of LPG, when the operating conditions (initial temperature and initial pressure) vary throughout the processing and utilization of LPG, the explosion characteristics of LPG will also change. However, the impact of the initial temperature and initial pressure on it needs to be enhanced. At the same time, the influence of the initial conditions on the key explosive characteristic factors has only been qualitatively studied, and no quantitative evaluation has been carried out. In this paper, a mathematical model of the LPG explosion in a confined space is developed based on the existing research. A study of the LPG−air mixture under different initial temperatures and pressure evaluated the explosion overpressure, explosion induction period, highest explosion pressure rising rate, and temperature. Finally, employing the fuzzy gray correlation analysis approach, the impacts of three parameters (initial temperature, initial pressure, and equivalent ratio) on the explosion characteristic factors of LPG are analyzed. The research findings may also be applied to determine the danger level of the explosion and formulate more efficient explosion prevention measures.

2. CALCULATION AND ANALYSIS METHOD

2.1. Calculation Method. In a confined space, the explosion process of combustible gas is a complicated chemical reaction accompanied by the flow. In this study, the Navier−Stokes equation is used to describe the gas-phase control equation, the gas-phase flow field is solved by a simple solver, the standard $k-\varepsilon$ model is utilized to describe the turbulent flow, and a simplified one-step reaction model is used to explain the explosion method of the combustible gas/air mixture. In this research, the computational fluid dynamics tool flame acceleration simulator (FLACS) version 10.3 was employed to solve the equation.[31] FLACS is the Renault Navier−Stokes three-dimensional solver generally recognized in the industry, which is broadly utilized in the numerical simulation of flammable gas and dust explosion. FLACS solves the Favre-averaged conservation equations for mass, momentum, enthalpy, turbulent kinetic energy, dissipation rate of turbulent kinetic energy, mass fraction of fuel, and mixture-fraction applying a finite volume method on a three-dimensional structured Cartesian grid. In Cartesian coordinates, the detailed governing equations are as follows:

Gas-phase model

$$\frac{\partial}{\partial t}(\beta_v \rho) + \frac{\partial}{\partial x_j}(\beta_j \rho u_j) = \frac{m}{V} \tag{1}$$

$$\frac{\partial}{\partial t}(\beta_v \rho u_i) + \frac{\partial}{\partial x_j}(\beta_j \rho u_i u_j) = -\beta_v \frac{\partial p}{\partial x_j} + \frac{\partial}{\partial x_j}(\beta_j \sigma_{ij}) + F_{o,i} + \beta_v F_{w,i} + \beta_v(\rho - \rho_0) g_i \tag{2}$$

$$\frac{\partial}{\partial t}(\beta_v \rho Y_{fuel}) + \frac{\partial}{\partial x_j}(\beta_j \rho u_j Y_{fuel}) = \frac{\partial}{\partial x_j}\left(\beta_j \frac{u_{eff}}{\sigma_{fuel}} \frac{\partial Y_{fuel}}{\partial x_j}\right) + R_{fuel} \tag{3}$$

where t is the time, s; β_v is the volumetric porosity; ρ is the gas-phase density, kg/m^3; x_j is the length in the j direction, m; β_j is the porosity in the direction; mass flow rate, kg/s; V is the volume, m;[3] u_i is the average velocity in the i direction, m/s; p is the absolute pressure, Pa; σ_{ij} is the stress tensor, N/m^2; $F_{o,i}$ is the flow resistance induced by obstacles in the i direction, Pa; ρ_0 is the initial density, kg/m^3; g_i is the gravitational acceleration in the I direction, m/s^2; h is the specific enthalpy, J/kg; μ_{eff} is the effective viscosity, Pa·s; D_p is the diffusion coefficient of particles; D_t is the diffusion coefficient of turbulence; Q is the heat dissipation, J/s; σ_h is the Plantt-Schmidt constant; Y_{fuel} is the mass fraction of fuel; and σ_{fuel} is the reaction rate of fuel, kg/m^3·s.

$$\frac{\partial}{\partial t}(\beta_v \rho k) + \frac{\partial}{\partial x_j}(\beta_j \rho u_i k) = \frac{\partial}{\partial x_j}\left(\beta_j \frac{u_{eff}}{\sigma_k} \frac{\partial k}{\partial x_j}\right) + \beta_v(P_k - \rho\varepsilon) \tag{4}$$

$$\frac{\partial}{\partial t}(\beta_v \rho\varepsilon) + \frac{\partial}{\partial x_j}(\beta_j \rho u_j \varepsilon) = \frac{\partial}{\partial x_j}\left(\beta_j \frac{u_{eff}}{\sigma_\varepsilon} \frac{\partial \varepsilon}{\partial x_j}\right) + \beta_v\left(P_\varepsilon - C_2 \rho \frac{\varepsilon^2}{k}\right) \tag{5}$$

The standard $k-\varepsilon$ model is employed to describe the gas flow field in this work. The k equation of turbulent kinetic energy and the ε equation of turbulent dissipation rate are calculated utilizing the model, which comprises two equations where k is the turbulent kinetic energy, m^2 s^{-2}; σ_k is the Plant-Schmidt constant of the turbulent kinetic energy; ε is the turbulent kinetic energy dissipation; and C_2 is the constant in the $k-\varepsilon$ equation, generally C_2 is 1.92. The combustion of propane and butane is reduced to an overall irreversible one-step reaction in this research.

In gas combustion, the finite rate/eddy current dissipation model is employed, and the mixed action of the chemical reaction and turbulence is considered at the same time. The actual reaction rate in the simulation is smaller than the Arrhenius reaction rate and the turbulent combined reaction rate.

2.2. Physical Models and Simulation Settings. As shown in Figure 1, the model comprises a closed pipe with a

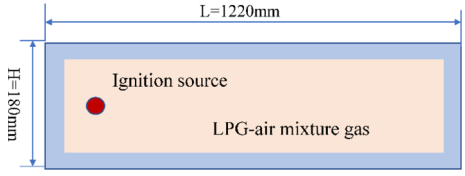

Figure 1. Simplified physical model diagram.

https://doi.org/10.1021/acsomega.1c03430
ACS Omega 2021, 6, 24683−24692

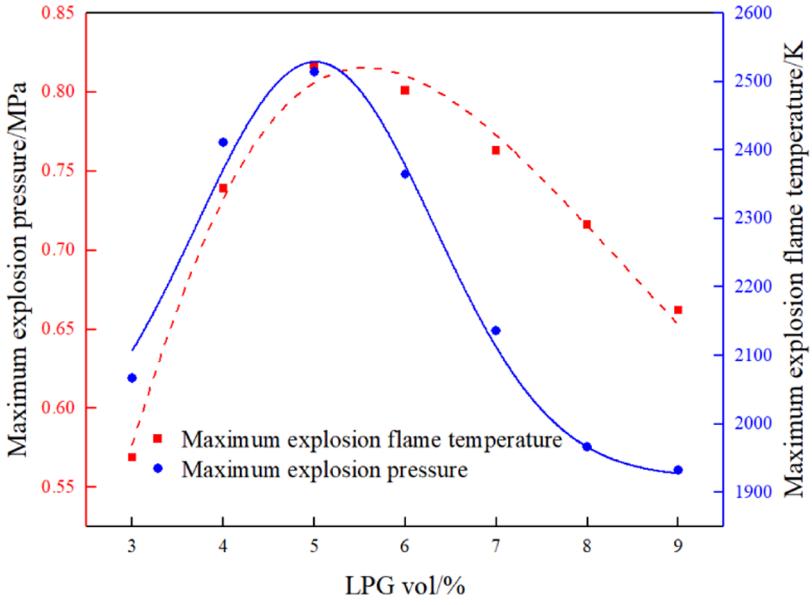

Figure 2. P_{max} and T_{max}.

length of 1220 mm, a width of 180 mm, a height of 180 mm, and a wall thickness of 25 mm. The numerical model and numerical grid applied in this work have been verified in previous work.[42,43] During the explosion reaction, the wall will disperse heat. The total explosion reaction, however, is faster (in milliseconds), and the wall heat dissipation is smaller. As a result, the heat dissipation effect of the pipe wall is negligible, and the wall surfaces are configured as non-slip adiabatic walls. The ignition source was 220 mm from the center of the closed end to the left, in a 6 mm radius spherical area. The reaction process variable $C = 1$ is set, to indicate the complete combustion of combustible gas in this region. The geometric model regions were generated employing hexahedral structured meshes. Four different numbers of grids (6.17×10^5, 1.83×10^5, 7.26×10^4, and 3.95×10^4) were utilized for the computation to ensure the independence of the grid and the convergence of the calculation findings. The results depict that with the further increase in the number of grids, the influence on the calculation findings can be negligible. Thus, the mesh generation scheme of 6.17×10^5 is chosen for the computation according to the comprehensive solution accuracy and computing power. In the process of numerical calculation, the iteration time step is set to 1×10^{-5}s. Each time step is set to 20 iterations, so that the calculation residual of each time step is less than 0.001. The entire area of the closed pipe is filled with a uniformly premixed LPG−air mixture. The main components of LPG are propane, butane, and a small number of olefins. In this paper, a mixture of 47% propane and 53% butane is used instead of LPG, which meets the composition requirements of LPG in GB11174-2011 and is universal and representative.[44]

2.3. Gray Relational Analysis. Gray relational analysis is a branch of gray system theory. The application of the gray relational analysis technique to evaluate things and phenomena impacted by several factors from the total concept is a generally acknowledged method.[45,46] The explosion characteristic parameters of combustible gases are closely linked to environmental factors. Nevertheless, the quantitative calculation of the correlation linking the two is still small. The gray correlation method is employed in this paper, to explore the internal relationship between initial temperature, initial pressure, equivalence ratio, and explosion characteristic parameters. This technique reveals the correlation between two variables with a minimal amount of data.

Step 1: the reference matrix and the comparison matrix are determined. The reference matrix can reflect the features of the system, which is expressed as follows

$$\mathbf{Y}_i = [y_i(1) y_i(2) y_i(3) \quad \cdots \quad y_i(n)] \qquad (i = 1, 2, 3) \tag{6}$$

A comparison matrix is a matrix composed of all the factors that influence the characteristics of the system. If the number of factors evaluated is m and these factors are investigated under n different conditions, the comparison matrix is demonstrated as follows:

$$x = \begin{bmatrix} x_1 \\ x_2 \\ \vdots \\ x_m \end{bmatrix} = \begin{bmatrix} x_1(1) & x_1(2) & \cdots & x_1(n) \\ x_2(1) & x_2(2) & \cdots & x_2(n) \\ \vdots & \vdots & \vdots & \vdots \\ x_m(1) & x_m(2) & \cdots & x_m(n) \end{bmatrix} \tag{7}$$

In this study, the explosion induction period (Y_1), the time to reach the maximum explosion pressure (Y_2), the highest explosion pressure (Y_3), and the maximum explosion pressure rise rate (Y_4) under different working conditions are considered as the reference matrix $y(k)$. Equivalence ratio, initial pressure, and temperature are selected to be the elements $x_1(k)$, $x_2(k)$, and $x_3(k)$ in the comparison matrix. The reference matrix and the comparison matrix are processed using eq 7.

Step 2: the dimensionless comparison matrix is obtained using the following formula

$$x_j(k)' = \frac{x_j(k) - \min x_j(k)}{\max x_j(k) - \min x_j(k)} \tag{8}$$

Step 3: the gray correlation coefficient is calculated

$$\xi_i(k) = \frac{\Delta_{min} + l \cdot \Delta_{max}}{\Delta(k) + l \cdot \Delta_{max}} \tag{9}$$

https://doi.org/10.1021/acsomega.1c03430
ACS Omega 2021, 6, 24683−24692

Step 4: the Euclid gray correlation level is calculated

$$W = (w_1, w_2, \cdots, w_t) \qquad t = 1, 2, \cdots, n \tag{10}$$

$$r'_{ij} = 1 - 2\sqrt{\sum_{k=1}^{n} [w(1 - \zeta_{ij}(k))]^2} \tag{11}$$

Step 5: the fuzzy gray correlation level is calculated. Using the results of steps 3 and 5, it can be calculated using the following formula

$$R_{ij} = \sqrt{\frac{r_{ij}^2 + (r'_{ij})^2}{2}} \tag{12}$$

Step 6: the influence of the investigation factors is sorted according to the size of the fuzzy gray correlation grade.

3. RESULTS AND DISCUSSION

3.1. Explosion Propagation Characteristics of LPG at Normal Temperature and Pressure. As seen in Figures 2 and 3, the highest explosion pressure rises with the increase in the LPG concentration. When the LPG concentration reaches 5%, the highest explosion pressure of LPG reaches a maximum of 0.817 MPa, and then, with the increase in the LPG concentration, the maximum explosion pressure decreases. Simultaneously, the change in law of the maximum explosion flame temperature (T_{max}) and the maximum explosion pressure rising rate is comparable to that of the maximum explosion pressure, which rises with the increase in the LPG volume fraction and reduces gradually when it reaches the highest point.

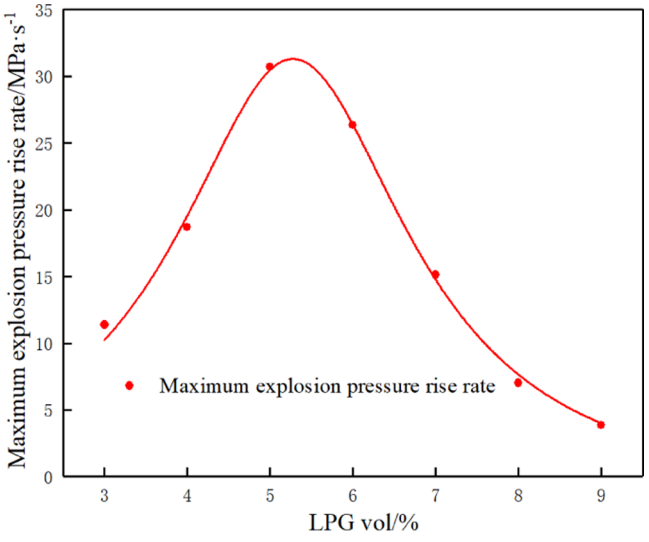

Figure 3. (dp/dt)max.

Figure 4 shows the temperature cloud distribution at four times (20, 30, 40, and 50 ms) in the process of explosion propagation using the numerical simulation results of 5% LPG as an example. As seen from Figure 4, after ignition, the flame travels from the ignition source to the wall. The flame propagation is moderately stable in the early stage of the reaction, and the flame combustion front propagates in a nearly spherical direction. With the growth of the reaction, the chemical reaction and turbulence jointly influence flame propagation. With the advancement in the flame to the wall, the limiting impact of the wall on the flame is also intensified. The flame combustion front propagates in two directions along the pipe wall[47] after it reaches the pipe wall. Therefore, in the later stage of the reaction, visible wrinkles are developed in the flame. The temperature of combustible gas in the pipeline tends to be consistent once the reaction is completed. The primary area in the pipeline can be divided into three: burned zone, preheated zone, and unburned zone.[48] The temperature of the unburned zone is the highest due to the exothermic reaction, and the temperature of the unburned zone does not increase at the initial stage of the reaction, but with the progress of the reaction, owing to the existence of thermal convection, the temperature of the unburned zone also rises slightly. A temperature transition zone, known as, the reaction preheating zone, exists between two regions, in which the combustible gas is heated, and participates in the chemical reaction at a higher temperature. The heat required to increase the temperature of the reaction preheating zone mainly comes from the heat discharge of the reaction, the heat conduction, and heat emission of the burned zone.

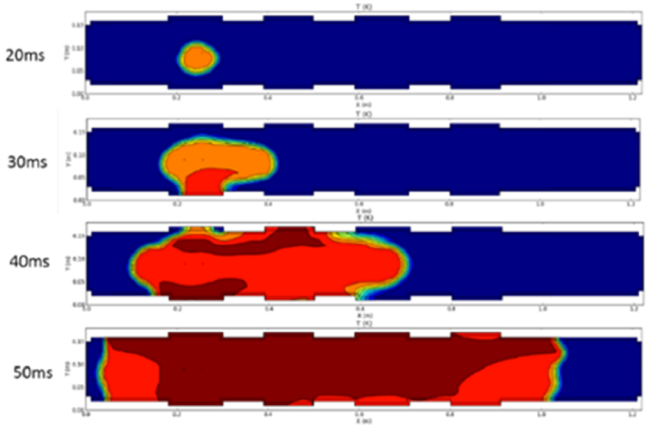

Figure 4. Structural evolution characteristics of LPG−air mixture explosion flame.

3.2. Influence of Initial Temperature and Pressure on the Explosion Pressure Parameters of LPG. The explosion propagation method of the LPG−air mixture with a 5% volume fraction in the pipeline under different initial temperatures (293−453 K) and initial pressure (0.1−1.0 MPa) is simulated. Figure 5 depicts the maximum explosion pressure and the time to achieve the maximum explosion pressure in the process of explosion propagation of the LPG−air mixture. The maximum explosion pressure reduces with the increase in initial temperature, the reaction rate rises with the increase in temperature, and the time to reach the maximum explosion pressure reduces with the increase in temperature.

After the ignition source acts on the LPG−air mixture, the strong explosion reaction does not occur immediately when the ignition source acts on the LPG−air combination; instead, the pressure starts to rise rapidly after a period, which is known as the explosion induction period. The explosion suppression technology study is based on determining the explosion induction period. The explosion sensor can be defined in several ways. The explosion sensor's end time might be when the pressure wave begins to rise, when the pressure increase rate reaches a certain value, or when the concentration of a specific component changes. The time taken for the pressure to rise to 7% in this paper is referred to as the explosion induction period. The explosion induction period is slowly

https://doi.org/10.1021/acsomega.1c03430
ACS Omega 2021, 6, 24683−24692

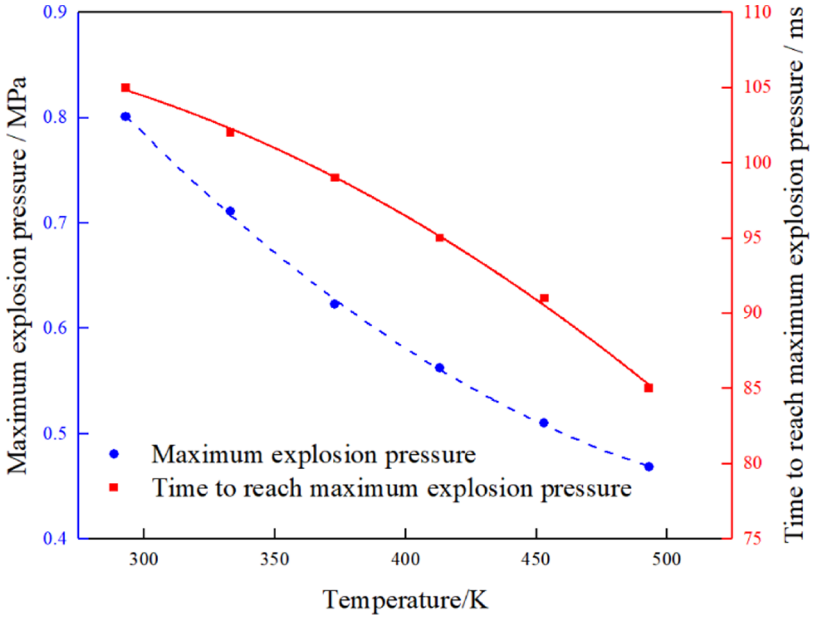

Figure 5. Explosion characteristic parameters of LPG at different initial temperatures.

shortened as the initial temperature, from 37 ms at 293 K to 21 ms at 453 K, as displayed in Figure 6. When the initial

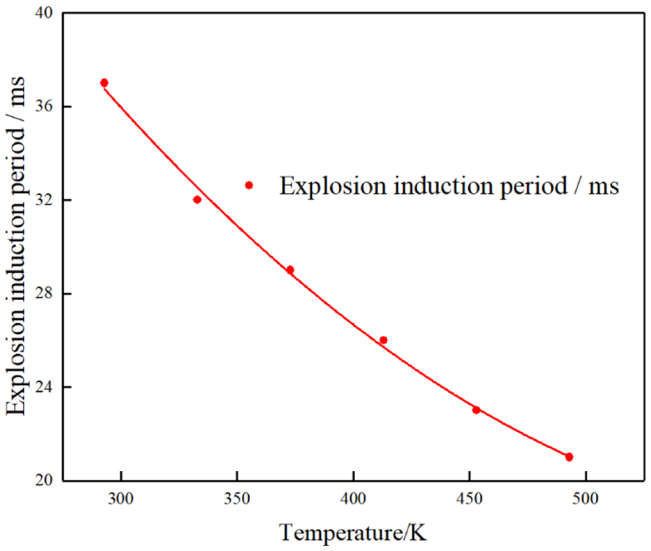

Figure 6. Explosion induction period of LPG at different initial temperatures.

temperature rises, the percentage of activated molecules in the reactants increases, and more reactant molecules participate in the initial reaction According to the Arrhenius empirical formula, as the temperature rises, the reaction rate constant increases, and the reaction rate accelerates, so the reaction can attain the rapid reaction stage faster, and the explosion induction period shortens with the increase in temperature.

The mixed gas is frequently subjected to complex working conditions (initial temperature, initial pressure, and equivalence ratio), throughout the production process, resulting in a more complicated change in its explosion features. The propagation of LPG explosion in the closed pipe is examined in this study under different initial temperatures (293−453 K), different initial pressures (0.1, 0.5, and 1.0 MPa), and different equivalence ratios (0.6, 0.8, 1.0, 1.2, and 1.4).

Research by Razus et al. showed that under certain conditions of temperature and fuel/oxygen ratio, the maximum explosion pressure is a linear function of the initial pressure. At the same time, when the initial pressure and fuel composition are constant, the explosion pressure decreases with the increase in the initial temperature.[19] The same conclusion was obtained in this work. Figure 7a depicts that the maximum explosion pressure increases linearly with the increase in initial pressure and reduces linearly with the increase in initial temperature. The distance between molecules decreases as the initial pressure increases. The number of colliding molecules increases, which speeds up the chemical reaction and promotes the increase in explosion pressure. Subsequently, the rise in explosion pressure accelerates the chemical reaction rate, thus increasing the total chemical reaction rate.[49−51] When the initial pressure is 0.1 MPa and the initial temperature increases from 293 to 453 K, the maximum explosion pressure decreases from 7.628 to 4.854 MPa.

Figure 7b illustrates that the time to reach the maximum explosion pressure decreases with the increase in the initial temperature at a lower initial pressure (P = 0.1 MPa). This is consistent with the conclusion of Liu et al.:[52] with the increase in the initial temperature, the flame propagation speed and reaction rate are increased; thus, the time to reach the maximum explosion pressure is shortened.

Figure 7c demonstrates that while the initial temperature is constant, the temperature of the explosion flame rises gradually with the increase in P. At the same time, when the initial outlet temperature increases, the impact of increasing the unit of P on the explosion flame temperature diminishes, indicating that the explosion flame has reached a threshold. It also reveals that when the initial pressure and temperature rises, the explosion flame temperature of the mixed fuel does not increase indefinitely.

Figure 7d indicates the three-dimensional evolution surface of the maximum explosion pressure under the coupling of initial temperature and pressure, from which the polynomial

https://doi.org/10.1021/acsomega.1c03430
ACS Omega 2021, 6, 24683−24692

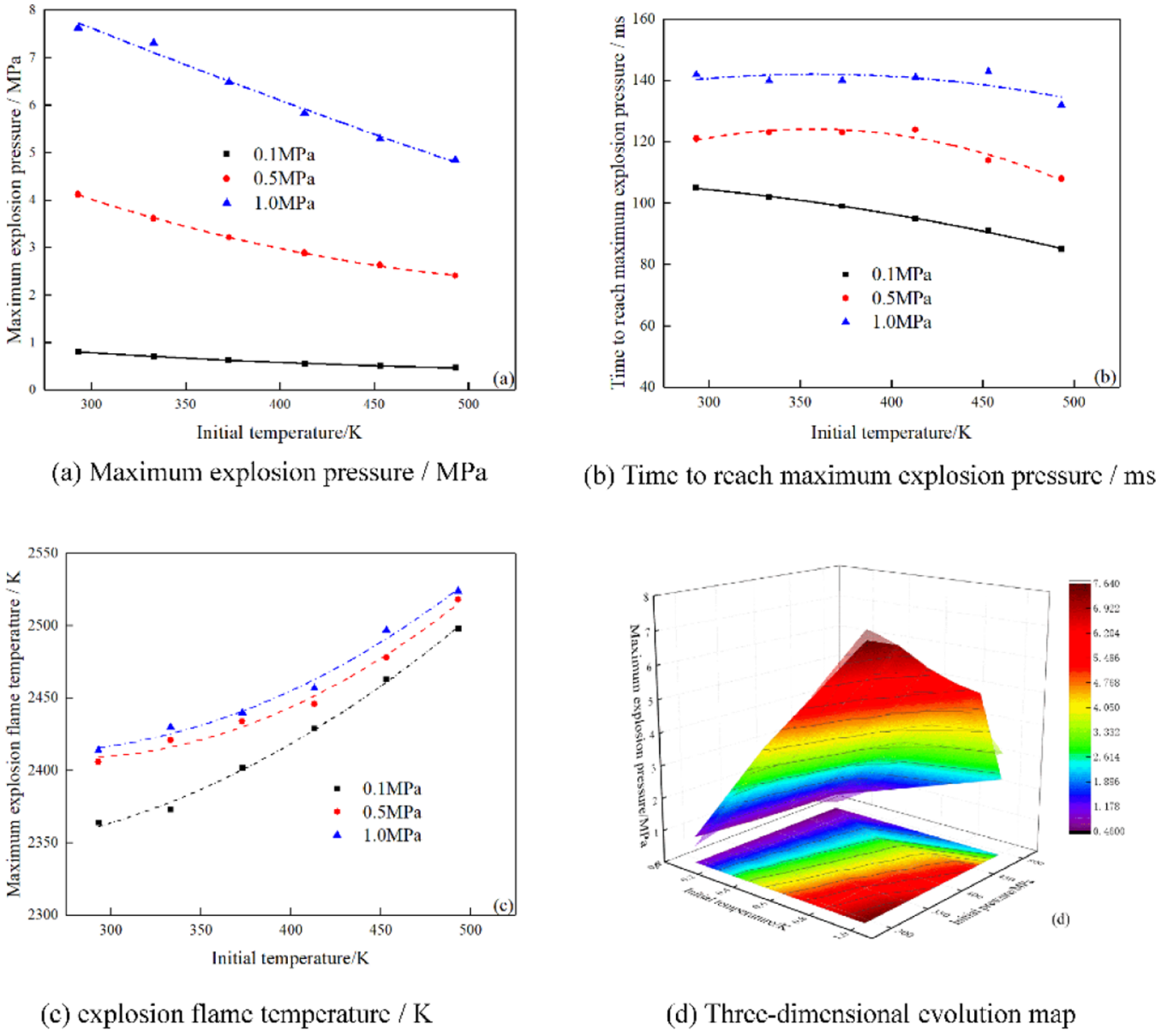

Figure 7. Explosion characteristics of LPG at different initial temperatures and pressures.

surface fitting function is obtained, as shown in formula 15. R^2 is 0.9717.

$$z = z_0 + ax + by + cx^2 + dy^2 + fxy \quad (13)$$

where $z_0 = -7.72208$, $a = 15.7471$, $b = 0.03966$, $c = -0.41275$, $d = -4.94641 \times 10^{-5}$, and $f = -0.02417$.

3.3. Effect of Initial Temperature and Pressure Coupling on the Explosion Propagation Law of LPG.

Figure 8 demonstrates the temperature field at the highest section of the pipeline at various initial temperatures at different times in the process of explosion propagation. As seen from the diagram, at the same time, owing to the increase in the initial temperature, the reaction is accelerated, and at the same time, the flame propagation distance becomes larger, that is, the flame propagation speed is accelerated. It can be discovered through comparative analysis that temperature rises, the combustion rate of LPG increases, and the propagation range of burned area increases substantially under the condition of high temperature. In addition, as seen from the diagram, when the initial temperature increases by 40 K, the temperature in the burning zone increases more than 40 K, so it can be concluded that the initial temperature does not affect the explosion temperature through simple accumulation. The comprehensive effect on the reaction rate and end-flow is primarily responsible for the complicated effect on the explosion process. Nevertheless, because of its extensive influence on the reaction rate and end-flow, it has a complicated impact on the explosion process. At the same time, the diagram shows that the temperature has a major impact on the transformation of the front structure of the flame. Many researchers are concerned about the propagation of premixed flame in the pipeline. The flame front shape changes from convex to concave as it propagates down the pipe, and this concave flame shape is named "tulip" flame. The production and propagation of tulip flame in the pipeline can be decomposed into the stage of flame spreading outward freely, and the front of flame evolves into the finger stage according to the development and evolution of the flame form.

https://doi.org/10.1021/acsomega.1c03430
ACS Omega 2021, 6, 24683−24692

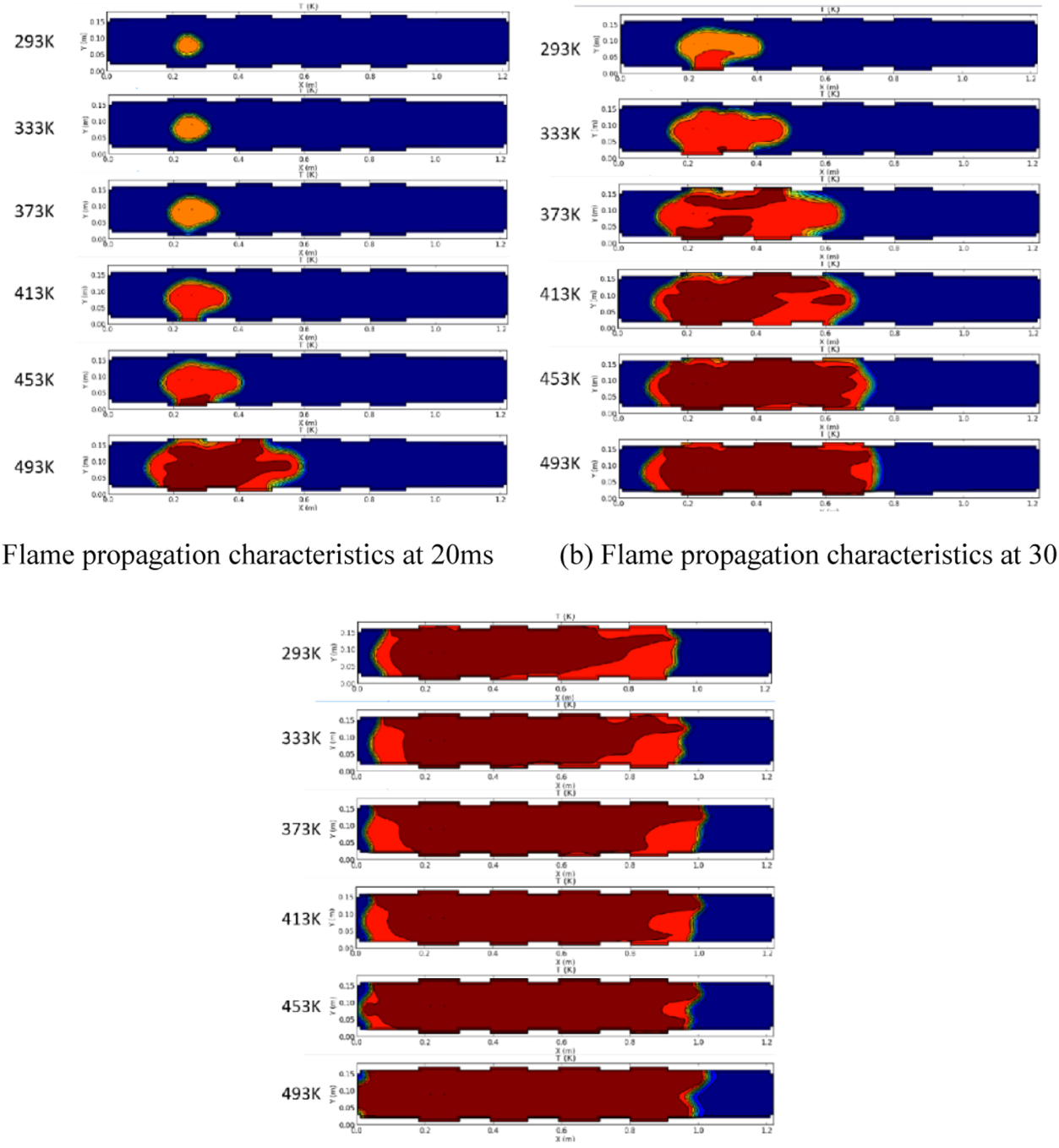

Figure 8. Structural evolution characteristics of LPG−air mixture explosion flame at different initial temperatures.

When the flame surface comes in contact with the sidewall, it forms a plane flame and finally transforms into a tulip flame.[10,11] As shown in Figure 8, the structure of the flame front has experienced the change in "spherical flame-finger flame-tulip flame" under various operating conditions. The following factors contributed to the emergence of tulip flames. However, the flame front sags inward in a closed pipeline due to reflected pressure waves. The flame near the wall surface, on the other hand, propagates faster than that at the axial center due to the impact of viscosity and turbulence on the tube wall, causing the tulip flame to extend further. With the increase in the initial temperature, the formation time of the tulip flame was advanced, and the depression of the flame front increased.

Figure 9 represents the transient temperature field in the pipeline at different initial pressures and temperatures. The propagation velocity of the flame is greatly affected by the pressure. In the initial stage of the reaction, the flame travels a longer distance at the same time. With the continuation of the reaction, when the initial pressure is low, the flame front with high initial temperature propagates a longer distance than the flame front with low initial temperature, that is, the burned zone at a higher temperature is much wider than that at a lower

https://doi.org/10.1021/acsomega.1c03430
ACS Omega 2021, 6, 24683−24692

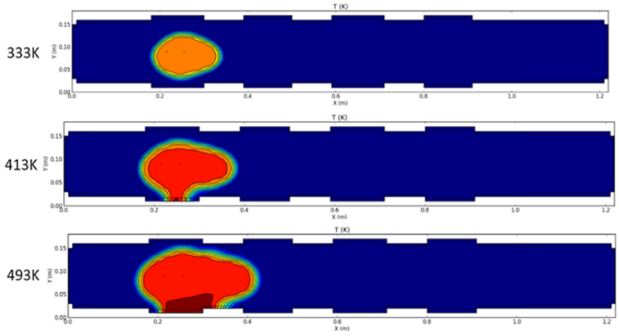

(b) Flame propagation characteristics at 20 ms and 1.0 MPa

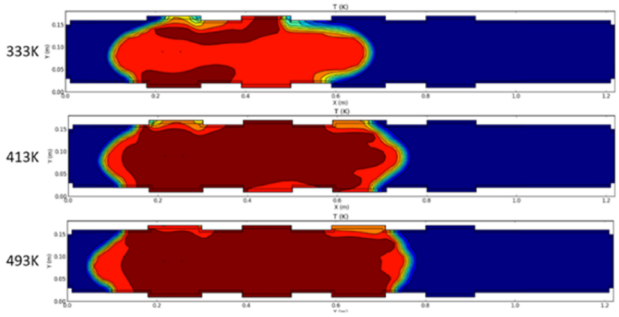

(c) Flame propagation characteristics at 30 ms and 0.5 MPa

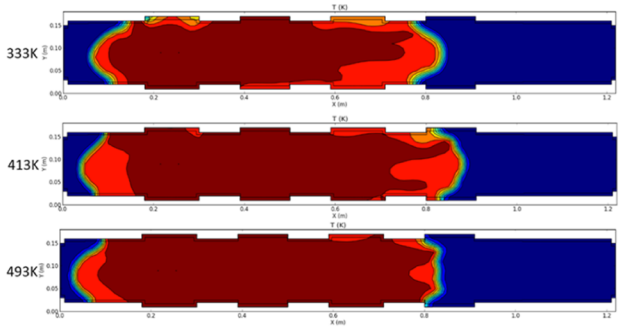

(d) Flame propagation characteristics at 30 ms and 1.0 MPa

Figure 9. Structural evolution of LPG−air mixture explosion flame under the combined action of initial temperature and pressure.

temperature. The influence of temperature on the flame propagation velocity when the initial pressure is greater than 0.5 MP is weakened due to the reflected pressure wave. As indicated in Figure 8, with the increase in initial pressure and temperature, the flame propagation speed and the transformation of the flame front structure are accelerated. When the initial temperature and pressure of the reaction system rise, some of the reaction systems exhibit lower-energy molecules, which absorb energy to become active molecules, increasing the fraction of active molecules in the entire reaction system. At the same time, the molecular activity is intense and regular under the condition of high temperature. It not only enlarges the number of molecular collisions in the reaction system but also increases the number of effective collisions. At the same time, the distance between molecules decreases with the increase in the initial pressure of the reaction system, and the probability of collision linking molecules enlarges because the distance amid molecules becomes shorter, and the collision times of molecules are also raised. The frequency factor in the reaction process is connected to the number of effective collisions. The frequency factor and the reaction rate constant increase as the number of effective collisions expands.

3.4. Gray Correlation Analysis. The explosion induction period ($Y1$), the time to reach the maximum explosion pressure ($Y2$), the maximum explosion pressure ($Y3$), and the maximum explosion pressure rise rate ($Y4$) are essential factors to evaluate the explosion risk.[52−54] These four parameters are regarded as the reference matrix, whereas the equivalent ratio, initial pressure, and initial temperature are utilized as the comparison matrix. The gray relational analysis approach is employed to solve the problem, according to Section 2.3. Figure 10 shows the computational findings, which demonstrate that the initial pressure has the largest influence on the four explosion parameters, and the fuzzy gray correlation grade is 0.59125, 0.61259, 0.77252, and 0.72865, respectively. The initial pressure is the major factor influencing the characteristics of explosion pressure according to gray correlation analysis. Therefore, in the process of using, storing, and transporting (LPG) mixed fuel, as well as related processing process design, more attention should be paid to the impact of initial pressure on explosion characteristics.

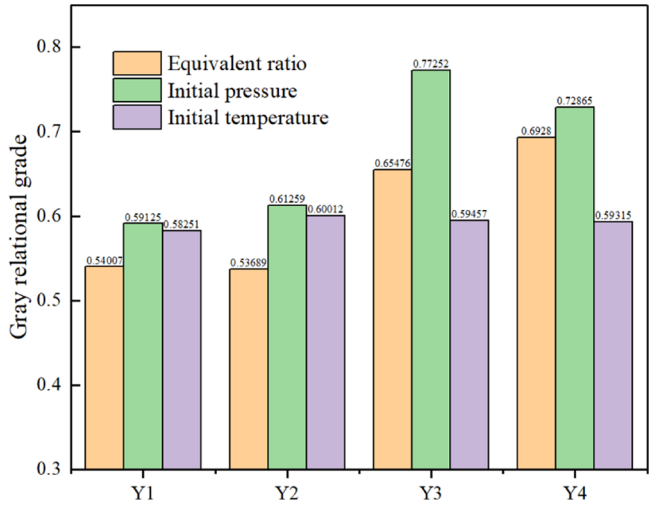

Figure 10. Gray relational grades.

4. CONCLUSIONS

In this paper, a mathematical model of LPG explosion in the enclosed space is established, and the features of explosion overpressure, explosion induction period, maximum explosion pressure rise rate, and flame propagation of LPG−air mixture at various initial temperatures and pressures are investigated. Simultaneously, employing the gray correlation analysis approach, the factors affecting the explosion characteristics are broadly examined. The findings indicate that the maximum explosion pressure and the increased rate of the maximum explosion pressure of the LPG−air mixture at room temperature rise with the increase in the LPG volume fraction and gradually reduce after reaching the highest value. With the rise in the initial temperature, the maximum explosion pressure and the explosion induction period decrease gradually. The maximum explosion pressure drops from 0.801 to 0.468

https://doi.org/10.1021/acsomega.1c03430
ACS Omega 2021, 6, 24683−24692

MPa when the initial temperature increases from 293 to 453 K. At the same time, the explosion induction period was reduced from 37 to 21 ms. In addition, the initial temperature has a great impact on the transformation of the flame front-end structure. The tulip flame formation time is accelerated, and the depression degree of the flame front increases as the initial temperature rises. When the initial pressure increases, the maximum explosion pressure increases with the increase in the initial pressure. At the same time, the explosion flame temperature increases gradually with the increase in the initial pressure, but when the initial pressure exceeds 0.5 MPa, its impact on the flame temperature gradually deteriorates. The gray relational analysis findings depict that the initial pressure has the highest effect on the four explosion parameters, and the gray relational degrees are 0.59125, 0.61259, 0.77252, and 0.72865, respectively. The results reveal the explosion pressure characteristics and flame propagation law of LPG in the confined space, which is efficient to the formulation of relevant industry standards and the development of scientific and effective explosion prevention measures. At the same time, it is extremely beneficial to the design of the explosion suppression approach and the further development of explosion accident consequence investigation.

The impact of two or more elements on explosion coupling can comprehensively analyze the effect of different factors on LPG explosion. However, this paper only looked at the coupling impact of initial temperature and pressure on explosion characteristics within a specific range of temperature and pressure. In future research work, we will further study the coupling effects of obstacles, gas compositions, and other factors on explosion characteristics.

AUTHOR INFORMATION

Corresponding Authors

Tao Wang − *School of Safety Science and Engineering, Xi'an University of Science and Technology, Xi'an 710054 Shaanxi, PR China;* orcid.org/0000-0002-1413-6270; Email: christfer@xust.edu.cn

Zhenmin Luo − *School of Safety Science and Engineering, Xi'an University of Science and Technology, Xi'an 710054 Shaanxi, PR China; Shaanxi Engineering Research Center for Industrial Process Safety & Emergency Rescue, Xi'an 710054 Shaanxi, PR China;* orcid.org/0000-0001-5247-9656; Email: zmluo@xust.edu.cn

Authors

He Liang − *School of Safety Science and Engineering, Xi'an University of Science and Technology, Xi'an 710054 Shaanxi, PR China*

Xuqing Wang − *School of Safety Science and Engineering, Xi'an University of Science and Technology, Xi'an 710054 Shaanxi, PR China*

Xiaofeng Kang − *School of Safety Science and Engineering, Xi'an University of Science and Technology, Xi'an 710054 Shaanxi, PR China*

Jun Deng − *Shaanxi Key Laboratory of Prevention and Control of Coal Fire, Xi'an 710054 Shaanxi, PR China*

Complete contact information is available at: https://pubs.acs.org/10.1021/acsomega.1c03430

Notes

The authors declare no competing financial interest.

ACKNOWLEDGMENTS

This work has been supported by the National Natural Science Foundation of China (grant nos. 52004208 and 51674193), the China Postdoctoral Science Foundation (grant no. 2019M663780), the Foundation of Shaanxi Educational Committee (grant no. 20JK0775), the Innovation Capability Support Program of Shaanxi (grant no. 2020TD021), and the Joint Foundation of Shaanxi (grant no. 2019JLM9). In addition, H.L. wants to especially thank T.W. and Z.L. for their strong support for the writing of this paper and Li Xi and Jin Kaiyan for their help in data processing.

REFERENCES

(1) Zhang, Q.; Wang, Y.; Lian, Z. Explosion hazards of LPG-air mixtures in vented enclosure with obstacles. *J. Hazard. Mater.* **2017**, *334*, 59−67.

(2) Raslavičius, L.; Keršys, A.; Mockus, S.; Keršienė, N.; Starevičius, M. Liquefied petroleum gas (LPG) as a medium-term option in the transition to sustainable fuels and transport. *Renewable Sustainable Energy Rev.* **2014**, *32*, 513−525.

(3) Woo, S.; Baek, S.; Lee, K. On-board LPG reforming system for an LPG · hydrogen mixed combustion engine. *Int. J. Hydrogen Energy* **2020**, *45*, 12203−12215.

(4) Chen, Y.; Zhang, Q.; Li, M.; Yuan, M.; Wu, D.; Qian, X. Experimental study on explosion characteristics of DME-blended LPG mixtures in a closed vessel. *Fuel* **2019**, *248*, 232−240.

(5) Wang, Y.; Lian, Z.; Zhang, Q. Effect of Ignition Location and Vent on Hazards of Indoor Liquefied Petroleum Gas Explosion. *Combust. Sci. Technol.* **2017**, *189*, 698−716.

(6) Razus, D.; Brinzea, V.; Mitu, M.; Oancea, D. Burning Velocity of Liquefied Petroleum Gas (LPG)−Air Mixtures in the Presence of Exhaust Gas. *Energy Fuels* **2010**, *24*, 1487−1494.

(7) Miao, J.; Leung, C. W.; Huang, Z.; Cheung, C. S.; Yu, H.; Xie, Y. Laminar burning velocities, Markstein lengths, and flame thickness of liquefied petroleum gas with hydrogen enrichment. *Int. J. Hydrogen Energy* **2014**, *39*, 13020−13030.

(8) Wang, T.; Zhou, Y.; Luo, Z.; Wen, H.; Zhao, J.; Su, B.; Cheng, F.; Deng, J. Flammability limit behavior of methane with the addition of gaseous fuel at various relative humidities. *Process Saf. Environ. Prot.* **2020**, *140*, 178−189.

(9) Wang, S.; Wu, D.; Guo, H.; Li, X.; Pu, X.; Yan, Z.; Zhang, P. Effects of concentration, temperature, ignition energy and relative humidity on the overpressure transients of fuel-air explosion in a medium-scale fuel tank. *Fuel* **2020**, *259*, 116265.

(10) Sun, X.; Lu, S. On the mechanisms of flame propagation in methane-air mixtures with concentration gradient. *Energy* **2020**, *202*, 117782.

(11) Yang, X.; Yu, M.; Zheng, K.; Wan, S.; Wang, L. A comparative investigation of premixed flame propagation behavior of syngas-air mixtures in closed and half-open ducts. *Energy* **2019**, *178*, 436−446.

(12) Di Sarli, V.; Di Benedetto, A.; Russo, G. Large Eddy Simulation of transient premixed flame−vortex interactions in gas explosions. *Chem. Eng. Sci.* **2012**, *71*, 539−551.

(13) Di Sarli, V.; Di Benedetto, A.; Russo, G. Sub-grid scale combustion models for large eddy simulation of unsteady premixed flame propagation around obstacles. *J. Hazard. Mater.* **2010**, *180*, 71−78.

(14) Di Sarli, V.; Di Benedetto, A.; Russo, G.; Jarvis, S.; Long, E. J.; Hargrave, G. K. Large Eddy Simulation and PIV Measurements of Unsteady Premixed Flames Accelerated by Obstacles. *Flow, Turbul. Combust.* **2009**, *83*, 227−250.

(15) Yu, M.; Fu, Y.; Zheng, L.; Pan, R.; Wang, X.; Yang, W.; Jin, H. Study on the combined effect of duct scale and SBC concentration on duct-vented methane-air explosion. *Process Saf. Environ. Prot.* **2021**, *148*, 939−949.

(16) Schiavetti, M.; Carcassi, M. N. Experimental tests of inhomogeneous hydrogen deflagrations in the presence of obstacles. *Int. J. Hydrogen Energy* **2021**, *46*, 12455−12463.
(17) Li, Y.; Bi, M.; Zhou, Y.; Jiang, H.; Huang, L.; Zhang, K.; Gao, W. Experimental and theoretical evaluation of hydrogen cloud explosion with built-in obstacles. *Int. J. Hydrogen Energy* **2020**, *45*, 28007−28018.
(18) Park, J.-W.; Oh, C. B. Flame structure and global flame response to the equivalence ratios of interacting partially premixed methane and hydrogen flames. *Int. J. Hydrogen Energy* **2012**, *37*, 7877−7888.
(19) Razus, D.; Brinzea, V.; Mitu, M.; Oancea, D. Temperature and pressure influence on explosion pressures of closed vessel propane−air deflagrations. *J. Hazard. Mater.* **2010**, *174*, 548−555.
(20) Cammarota, F.; Di Benedetto, A.; Di Sarli, V.; Salzano, E. Influence of initial temperature and pressure on the explosion behavior of n-dodecane/air mixtures. *J. Loss Prev. Process Ind.* **2019**, *62*, 103920.
(21) Grabarczyk, M.; Teodorczyk, A.; Di Sarli, V.; Di Benedetto, A. Effect of initial temperature on the explosion pressure of various liquid fuels and their blends. *J. Loss Prev. Process Ind.* **2016**, *44*, 775−779.
(22) Salzano, E.; Cammarota, F.; Di Benedetto, A.; Di Sarli, V. Explosion behavior of hydrogen−methane/air mixtures. *J. Loss Prev. Process Ind.* **2012**, *25*, 443−447.
(23) Cammarota, F.; Di Benedetto, A.; Di Sarli, V.; Salzano, E.; Russo, G. Combined effects of initial pressure and turbulence on explosions of hydrogen-enriched methane/air mixtures. *J. Loss Prev. Process Ind.* **2009**, *22*, 607−613.
(24) Huzayyin, A. S.; Moneib, H. A.; Shehatta, M. S.; Attia, A. M. A. Laminar burning velocity and explosion index of LPG−air and propane−air mixtures. *Fuel* **2008**, *87*, 39−57.
(25) Huo, Y.; Chow, W. K. Flame propagation of premixed liquefied petroleum gas explosion in a tube. *Appl. Therm. Eng.* **2017**, *113*, 891−901.
(26) Li, Y.; Bi, M.; Li, B.; Zhou, Y.; Gao, W. Effects of hydrogen and initial pressure on flame characteristics and explosion pressure of methane/hydrogen fuels. *Fuel* **2018**, *233*, 269−282.
(27) Chen, S.; Shen, H.; Zhu, Q.; Liang, D. Effect of initial temperature and initial pressure on vapor explosion characteristics of nitro-thinner. *J. Loss Prev. Process Ind.* **2019**, *61*, 298−304.
(28) Sun, K.; Zhang, Q. Experimental study of the explosion characteristics of isopropyl nitrate aerosol under high-temperature ignition source. *J. Hazard. Mater.* **2021**, *415*, 125634.
(29) Heilbronn, D.; Barfuss, C.; Sattelmayer, T. Influence of geometry on flame acceleration and DDT in H2-CO-air mixtures in a partially obstructed channel. *J. Loss Prev. Process Ind.* **2021**, *71*, 104493.
(30) Huang, C.; Chen, X.; Liu, L.; Zhang, H.; Yuan, B.; Li, Y. The influence of opening shape of obstacles on explosion characteristics of premixed methane-air with concentration gradients. *Process Saf. Environ. Prot.* **2021**, *150*, 305−313.
(31) Chen, G.; Ling, X.; Zheng, Y.; Gu, M.; Wang, H.; Yu, A. Propane-air mixture deflagration hazard with different ignition positions and restraints in large-scale venting chamber. *J. Loss Prev. Process Ind.* **2021**, *71*, 104520.
(32) Di Sarli, V.; Di Benedetto, A.; Russo, G. Using Large Eddy Simulation for understanding vented gas explosions in the presence of obstacles. *J. Hazard. Mater.* **2009**, *169*, 435−442.
(33) Yang, W.; Zheng, L.; Wang, C.; Wang, X.; Jin, H.; Fu, Y. Effect of ignition position and inert gas on hydrogen/air explosions. *Int. J. Hydrogen Energy* **2021**, *46*, 8820−8833.
(34) Yao, Z.; Deng, H.; Dong, J.; Wen, X.; Zhang, X.; Wang, F.; Chen, G. On explosion characteristics of premixed syngas/air mixtures with different hydrogen volume fractions and ignition positions. *Fuel* **2020**, *288*, 119619.
(35) Wang, H.; Gu, S.; Chen, T. Experimental Investigation of the Impact of CO, C2H6, and H2 on the Explosion Characteristics of CH4. *ACS Omega* **2020**, *5*, 24684−24692.
(36) Hamidi, N.; Ilminnafik, N. Inert Effects on Flammability Limits and Flame Propagation of LPG by CO2. *Appl. Mech. Mater.* **2014**, *664*, 226−230.
(37) Salzano, E.; Basco, A.; Cammarota, F.; Di Sarli, V.; Di Benedetto, A. Explosions of Syngas/CO2 Mixtures in Oxygen-Enriched Air. *Ind. Eng. Chem. Res.* **2012**, *51*, 7671−7678.
(38) Di Benedetto, A.; Cammarota, F.; Di Sarli, V.; Salzano, E.; Russo, G. Reconsidering the flammability diagram for CH4/O2/N2 and CH4/O2/CO2 mixtures in light of combustion-induced Rapid Phase Transition. *Chem. Eng. Sci.* **2012**, *84*, 142−147.
(39) Yasiry, A. S.; Shahad, H. A. K. An experimental study of the effect of hydrogen blending on burning velocity of LPG at elevated pressure. *Int. J. Hydrogen Energy* **2016**, *41*, 19269−19277.
(40) Zhang, Q.; Chen, Y.; Fan, T.; Yuan, M.; Liu, Z.; Huang, P.; Qian, X. Flame dynamics and flammability limit of DME(30%)/LPG blended clean fuel in elongated closed pipeline under multi-factors. *Fuel* **2019**, *254*, 115731.
(41) Gexcon. *FLACS v10.7 User's Manual, Norway*, 2017.
(42) Su, B.; Luo, Z.-m.; Wang, T.; Liu, L. Experimental and numerical evaluations on characteristics of vented methane explosion. *J. Cent. South Univ.* **2020**, *27*, 2382−2393.
(43) Luo, Z.; Hao, Q.; Wang, T.; Li, R.; Cheng, F.; Deng, J. Experimental study on the deflagration characteristics of methane-ethane mixtures in a closed duct. *Fuel* **2020**, *259*, 116295.
(44) Committee, C. N. S. M. Liquefied petroleum gases. http://c.gb688.cn/bzgk/gb/showGb?type=online&hcno=5C74EF28180CB01DC81DF7A757CED08A (accessed 2020.07.05).
(45) E, J.; Zeng, Y.; Jin, Y.; Zhang, B.; Huang, Z.; Wei, K.; Chen, J.; Zhu, H.; Deng, Y. Heat dissipation investigation of the power lithium-ion battery module based on orthogonal experiment design and fuzzy grey relation analysis. *Energy* **2020**, *211*, 118596.
(46) Zuo, W.; E, J.; Liu, X.; Peng, Q.; Deng, Y.; Zhu, H. Orthogonal Experimental Design and Fuzzy Grey Relational Analysis for emitter efficiency of the micro-cylindrical combustor with a step. *Appl. Therm. Eng.* **2016**, *103*, 945−951.
(47) Zhang, F.; Zirwes, T.; Häber, T.; Bockhorn, H.; Trimis, D.; Suntz, R. Near Wall Dynamics of Premixed Flames. *Proc. Combust. Inst.* **2020**, *38*, 1955−1964.
(48) Jing, Q.; Huang, J.; Liu, Q.; wang, D.; Chen, X.; Wang, Z.; Liu, C. The flame propagation characteristics and detonation parameters of ammonia/oxygen in a large-scale horizontal tube: As a carbon-free fuel and hydrogen-energy carrier. *Int. J. Hydrogen Energy* **2021**, *46*, 19158−19170.
(49) Varghese, R. J.; Kolekar, H.; Kishore, V. R.; Kumar, S. Measurement of laminar burning velocities of methane-air mixtures simultaneously at elevated pressures and elevated temperatures. *Fuel* **2019**, *257*, 116120.
(50) Wang, S.; Wang, Z.; Elbaz, A. M.; Han, X.; He, Y.; Costa, M.; Konnov, A. A.; Roberts, W. L. Experimental study and kinetic analysis of the laminar burning velocity of NH3/syngas/air, NH3/CO/air and NH3/H2/air premixed flames at elevated pressures. *Combust. Flame* **2020**, *221*, 270−287.
(51) Yang, X.; Yu, M.; Zheng, K.; Luan, P.; Han, S. An experimental study on premixed syngas/air flame propagating across an obstacle in closed duct. *Fuel* **2020**, *267*, 117200.
(52) Liu, Y.; Zhang, Y.; Zhao, D.; Yin, J.; Liu, L.; Shu, C.-M. Experimental study on explosion characteristics of hydrogen−propane mixtures. *Int. J. Hydrogen Energy* **2019**, *44*, 22712−22718.
(53) Tang, C.; Zhang, S.; Si, Z.; Huang, Z.; Zhang, K.; Jin, Z. High methane natural gas/air explosion characteristics in confined vessel. *J. Hazard. Mater.* **2014**, *278*, 520−528.
(54) Wang, T.; Luo, Z.; Wen, H.; Cheng, F.; Liu, L.; Su, Y.; Liu, C.; Zhao, J.; Deng, J.; Yu, M. The explosion enhancement of methane-air mixtures by ethylene in a confined chamber. *Energy* **2021**, *214*, 119042.

https://doi.org/10.1021/acsomega.1c03430
ACS Omega 2021, 6, 24683−24692